

Two *s*-wave solutions for superconductivity in the extended Hubbard model

Maciej Bak*

Institute of Physics, A. Mickiewicz University, Umultowska 85, 61-614 Poznań, Poland

The existence of more than one solution for *s*-wave pairing in the extended Hubbard model is not often realized. This possibility was noted by Friedberg *et al.* [Phys. Rev. B50, 10190 (1994)] in the case of two electrons on a lattice, without further analysis. In the present paper, the second solution is found also in the case of superconductivity of extended *s*-wave symmetry in the extended Hubbard model. The properties of both *s*-wave solutions are examined by mean-field methods and thresholds for their appearance are given. A possibility of the first-order transition is discovered and modifications of the phase diagram are calculated. Results of this paper in the limit of low electron density are also applicable to the bound, two-electron pairs.

PACS numbers: 74.20.Fg, 71.10.Fd, 74.20.Rp

I. INTRODUCTION

The discovery of high-temperature superconductivity (HTS) has triggered an intensive effort to reveal its mechanisms. This aim has not been attained yet but the amount of knowledge concerning HTS is substantial. From this wealth of data certain key issues emerge, which must be addressed by the eventual microscopic theory. One of them is question of the symmetry of the order parameter. Instead of originally accepted *s*-wave, nowadays it is believed that the hole-doped HTS materials are predominantly of the $d_{x^2-y^2}$ -wave symmetry.^{1,2} Nevertheless the research concerning the *s*-wave symmetry is not to be abandoned. The *s*-wave symmetry is found in fullerides,³ perovskites⁴ and MgB_2 ,⁵ not from the HTS group but very interesting materials though. The order parameter of *s* symmetry can appear as subdominant one in *d*-wave superconductors due to orthorombic distortions of the crystal.^{6,7,8} There is evidence of the *s* type HTS in electron-doped materials^{9,10,11,12} and possibility of the *s* to *d* change of the symmetry of the order parameter with increasing doping in the hole-doped materials.^{13,14} Another scenario with *s*-wave symmetry includes the possibility of different order parameters in the bulk and on the surface of HTS superconductor.¹⁵ As there are reports of different mechanisms responsible for pairing and phase coherence there is possibility of pseudogap having *s* symmetry, different from the *d* symmetry of the order parameter.^{16,17} Of other possibilities we can not exclude possibility of finding an *s*-wave symmetry pairing in heavy fermions, which are notorious for multiplicity of phases.

There are few rigorous results concerning *s*-wave superconductivity or BCS in general. We know that in the dilute limit BCS mean-field equations go over to the Schrödinger equation for the bound two-electron pair,^{13,18} i.e. in this limit the BCS equations become *exact*. Another result was given by Randeria *et al.*¹⁹ stating that creating two-electron bound state of *s*-wave symmetry is a necessary and sufficient condition for BCS-type superconductivity to exist in two dimensions in a dilute limit. The results of applying mean-field approxi-

mations to the Hubbard-type Hamiltonians as well as the properties of the bound pairs are well known (e.g. Refs 13,20,21,22,23,24,25). One of the seldom noticed aspects of mean-field treatment of the extended *s*-wave pairing and bound pairs of this symmetry is subject of this paper.

II. FORMALISM

Let's consider extended Hubbard model in the standard notation:

$$H = \sum_{ij\sigma} (t_{ij} - \mu\delta_{ij}) c_{i\sigma}^\dagger c_{j\sigma} + U \sum_i n_{i\uparrow} n_{i\downarrow} + W \sum_{ij\sigma\sigma'} n_{i\sigma} n_{j\sigma'} \quad (1)$$

where we sum over nearest neighbors (n.n.), U and W are on- and intersite interactions respectively, t_{ij} is nearest-neighbor hopping integral and μ - chemical potential. In the mean-field approach the above Hamiltonian takes the form²⁶:

$$H = \sum_{k\sigma} (\varepsilon_k - \bar{\mu}) n_{k\sigma} - \sum_k (\Delta_k c_{k\uparrow}^\dagger c_{-k\downarrow}^\dagger + H.c.) + const. \quad (2)$$

where, using order parameter $\langle c_{-q\downarrow} c_{q\uparrow} \rangle$, we introduced a gap Δ_k :

$$\Delta_k = \frac{1}{N} \sum_q V_{kq} \langle c_{-q\downarrow} c_{q\uparrow} \rangle \quad (3)$$

$$V_{kq} = -U - W\gamma_{k-q} \quad (4)$$

$$\gamma_k = \sum_{\delta}^z \exp(i\mathbf{k} \cdot \boldsymbol{\delta}) \quad (5)$$

$$\varepsilon_k = -t\gamma_k \quad (6)$$

$$\bar{\mu} = \mu - (U/2 + Wz)n \quad (7)$$

z is coordination number; for the full discussion of the model the reader is referred to the Ref.²⁶ It is easy to derive the self-consistent equation for the energy gap:

$$\Delta_k = \frac{1}{N} \sum_q V_{kq} \frac{\Delta_q}{2E_q} \tanh \beta E_q / 2 \quad (8)$$

where the quasiparticle energy:

$$E_q = \sqrt{(\varepsilon_q - \bar{\mu})^2 + |\Delta_q|^2} \quad (9)$$

and $\beta = 1/(k_B T)$ where T is temperature and k_B Boltzmann constant. To solve the model we usually make the ansatz:¹³

$$\Delta_k = \Delta_0 + \Delta_\gamma \gamma_k + \Delta_\eta \eta_k \quad (10)$$

where $\eta_k = 2(\cos k_x - \cos k_y)$ and particular terms refer to on-site s -, extended s - and d -wave pairings. Self-consistent equations for the gap separate into the s -wave and d -wave part.

Finally what is left for solving for general, non-zero U and W in the ground state is a set of three self-consistent equations for Δ_0 , Δ_γ and chemical potential $\bar{\mu}$:

$$\Delta_0 = -U \frac{1}{N} \sum_q (\Delta_0 + \gamma_q \Delta_\gamma) \frac{1}{2E_q} \quad (11)$$

$$\Delta_\gamma = -\frac{W}{z} \frac{1}{N} \sum_q \gamma_q (\Delta_0 + \gamma_q \Delta_\gamma) \frac{1}{2E_q} \quad (12)$$

$$n - 1 = -\frac{1}{N} \sum_q \frac{(\varepsilon_q - \bar{\mu})}{E_q} \quad (13)$$

in the case of the extended s -wave pairing, and

$$1 = -\frac{W}{z} \frac{1}{N} \sum_q \eta_q^2 \frac{1}{2E_q} \quad (14)$$

in the case of the d -wave pairing. In the following we will focus on the s -wave pairing only. The results described in the remainder of the paper are calculated for the rectangular density of states (DOS) with $z = 4$, so they approximate two dimensional square lattice. For the reasons that will be explained later on the author supposes that they are of more general nature.

III. RESULTS

Equations (11)-(13) in the dilute limit yield Schrödinger equation for a bound pair, as was told in the Introduction. As is well known, in two dimensions infinitesimally small on-site attraction creates bound pair for $W = 0$. For $W > 0$ a threshold must be crossed to obtain a bound state. Analytic formula for the threshold and U - W phase diagram are given for example in.^{13,27} The less known facts are as follows:

(i) The threshold formula for the gap, analogical to the one given in,^{13,27} can be derived from BCS-MFA equations (11)-(13) *without* resorting to the limit $n \rightarrow 0$. Using rectangular density of states it reads:

$$\frac{W_{crit}}{4t} = \frac{-1}{1 + (n-1)^2 (1 + 16t/U)} \quad (15)$$

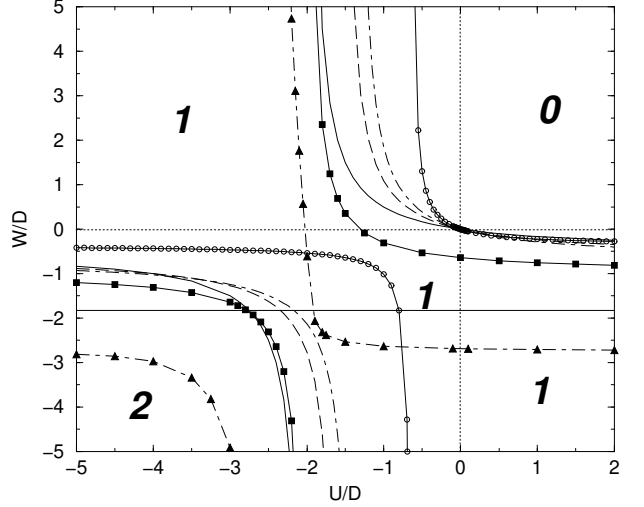


FIG. 1: Critical values for existence of extended s -wave superconductivity calculated for the rectangular DOS, for electron densities $n = 0$ (also $n = 2$, full line) and $n = 0.2$ (also $n = 1.8$, dashed line). Dot-dashed and full line with circles are thresholds for $n = 0.2$, calculated for the exact DOS in two dimensions (2d) and in three dimensions (3d, simple cubic lattice) respectively. Exact 2d threshold for $n = 0$ is the same as for rectangular DOS. Exact 3d threshold for $n = 0$ is given by solid line with squares. Dotted lines are the axes of coordination system. Dot-dashed lines with triangles are crossover boundaries for $n = 0.2$ and exact 2d DOS. Crossover boundaries for $n = 0$ coincide with the threshold lines in 2d. Full, flat, horizontal line is a threshold for the d -wave pairing, calculated for $n = 0$. Numbers "0", "1" and "2" are the names of the areas described in the text. U and W are in the half-bandwidth units $D = 4t$ in 2d and $D = 6t$ in 3d.

Let's note that the limit $n \rightarrow 0$ yields correct result of Refs.^{13,27} The use of the exact density of states does not bring changes to the value of W_{crit} for $n \rightarrow 0$ but the changes appear and increase with growing n , as shown in Fig. 1.

(ii) The formula (15) is valid on the *entire* U - W plane, both for positive and negative values of U and W . The cited papers show the figure of the fourth quarter of the coordination system only. The full plot is given in Fig. 1. As we can see in the third quarter of the coordination system, for U and W attractive enough, a second threshold line is obtained! (In the case of two-electron bound pair second solution was also noted in Ref.²⁵ but without further analysis).

This way the area in Fig. 1 can be divided into three main parts: Area "0" - to the right of the rightmost threshold line, mostly first quarter ($U > 0, W > 0$) and small parts of the second and fourth quarter of the coordination system (not exceeding asymptotic values: $U_{as}/t = -16(n-1)^2/(1+(n-1)^2)$ and $W_{as}/t = -4/(1+(n-1)^2)$). There are no bound states and no gap for these parameters, the solutions describe antibonding states. Area "1" - between both threshold lines, mostly second and fourth quarter - in this area there is only one solution of

the equations (11)-(13), which exists even for infinite on- or intersite repulsion. The further from the rightmost threshold line we are the stronger is the binding between electrons in the pairs. Points of the same binding energy form a line approximately parallel to the rightmost threshold line. Area "2" – below the second threshold line, in the third quarter – for parameters from this area two solutions of equations (11)-(13) exist: one of the type of the "area 1", with large binding energy, given by a "distance" from the first threshold line; the other, with smaller binding energy and smaller gap, given by the "distance" from the second threshold line. We will call these solutions type 1 and type 2, respectively. Let's note, that the range of U , for which both types of pairing exist, increase with increasing n (the asymptote moves from $U_{as}/4t = -2$ for $n = 0$ to $U_{as} = 0$ for $n = 1$) while analogical range of W decrease (the asymptote moves from $W_{as}/4t = -1/2$ for $n = 0$ to $W_{as}/4t = -1$ for $n = 1$). The properties of both types of pairing are described in the following.

For fixed W , for $U \rightarrow -\infty$, type 1 solution displays what we will call here "pure-s" type behavior: $|\Delta_0| \sim U$, $\Delta_\gamma \rightarrow 0$, $\bar{\mu} \sim U/2$ (if $W > 0$ then $\Delta_\gamma < 0$, if $W < 0$ then $\Delta_\gamma > 0$). When we move on the U axis from left to right, towards smaller values of $|U|$ then, for certain intermediate value of $|U|$ (not too large if W is not large and attractive) this "pure-s" behavior disappears. If $W > W_{as}$ then with increasing U we must reach threshold value U_{crit} and for $U \rightarrow U_{crit}$ Δ_0 decreases non-linearly to 0, $|\Delta_\gamma|$ goes through extremum and also decreases to 0 while $\bar{\mu}$ goes to constant, non-zero value. If $W < W_{as}$ and solution of type 1 exists in the whole range of U from $-\infty$ to $+\infty$, then for $U \rightarrow +\infty$ all three quantities Δ_0 , Δ_γ and $\bar{\mu}$ go to the constant values: Δ_0 to a small negative one and Δ_γ to a larger, positive one (see Fig. 2). When $W < 0$ and $|W|$ is large enough, then "pure-s" behavior disappears for $U \approx W$ instead of small to intermediate values of $|U|$, as shown in Fig. 2.

The behavior of type 2 solution is somewhat complementary: for $U \rightarrow -\infty$, when type 1 solution shows "pure-s" behavior, type 2 solution is constant. Moving right on the U axis type 2 solution goes through a transition for the same range of U as type 1 solution, and from now on it behaves in "pure-s" way until U reaches the threshold for type 2 solutions, where Δ_0 and Δ_γ disappear and $\bar{\mu} = \text{const}$. Let's note, that the slope of linear dependence of Δ_0 vs U differs just by the sign from the analogical slope of type 1 solution and that Δ_γ is of opposite sign to Δ_0 in type 2 solution.

The constant values reached by the type 1 solution for $U \rightarrow +\infty$ are the same as the ones reached by the type 2 solution for $U \rightarrow -\infty$. These constants for small n and $|W|$ large enough can be calculated as:

$$\bar{\mu} = W/2 \quad (16)$$

$$\Delta_\gamma/\Delta_0 = -|\bar{\mu}| \quad (17)$$

$$\Delta_0 \approx -0.6\sqrt{n} \quad (18)$$

As shown in Fig. 3 for fixed U , when W is varied, instead

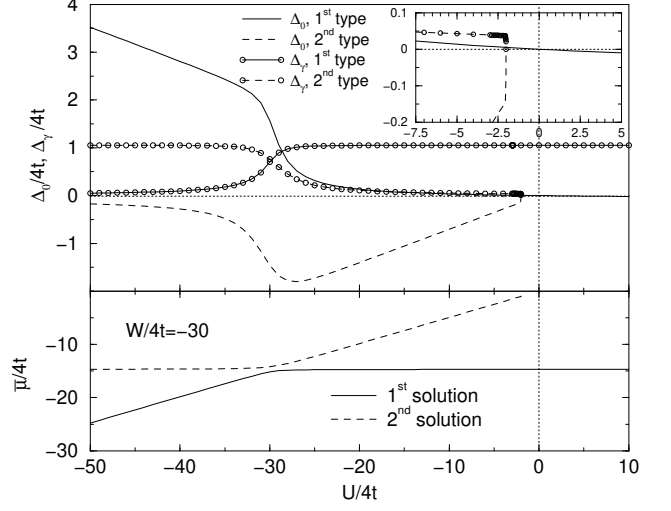


FIG. 2: Type 1 (full line, full line with circles) and type 2 (dashed line, dashed line with circles) solutions of the extended Hubbard model vs $U/4t$ for $W/4t = -30$ and $n = 0.01$. Upper panel shows Δ_0 and Δ_γ and lower panel $\bar{\mu}$. Dotted lines show axes of the coordination system. In the inset the enlargement of the area near the origin of the coordination system in the upper panel is shown.

of "pure-s" behavior type 1 solution displays "pure extended s" behavior for $W \rightarrow -\infty$: $\Delta_\gamma \sim |W|$, $\Delta_0 \rightarrow 0$, $\bar{\mu} \sim W/2$. Apart from that, the behavior of solutions vs W is analogous to the behavior of the solutions vs U : for $W \rightarrow +\infty$ type 1 solution goes to the constant values (now Δ_γ to the small negative one while Δ_0 to the bigger, positive one) and for $W \rightarrow -\infty$ type 2 solution goes to the same constants. For small n and $|U|$ large enough these constants are:

$$\bar{\mu} = U/2 \quad (19)$$

$$\Delta_0/\Delta_\gamma = -4|\bar{\mu}| \quad (20)$$

$$\Delta_\gamma \approx -\sqrt{n/8} \quad (21)$$

Large values of fixed parameters in Figs 2 and 3 were chosen to emphasize the characteristic behavior of the examined quantities. The plot of chemical potential $\bar{\mu}$ vs U for $W/4t = -30$ is practically indistinguishable from the plot of $\bar{\mu}$ vs W for $U/4t = -30$ in the scale of the picture (apart from the different critical values for which $\bar{\mu}$ in the type 2 solutions appears) so it was not shown again in Fig. 3.

A point to notice is that the gap parameter Δ_0 remains finite even in the limit $U \rightarrow \infty$, despite the fact that on-site pairing amplitude $\langle c_{i\uparrow}^\dagger c_{i\downarrow}^\dagger \rangle$ must vanish in this limit.^{28,29}

Let's note that the considerations above answer the unspoken question, why the equations for extended s -wave pairing yield formally (and numerically) the same solution in the two very different limits: infinite attraction and infinite on- or intersite repulsion. Despite they are

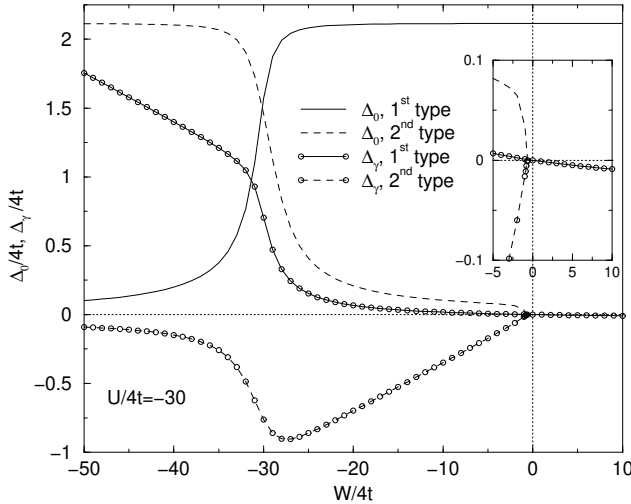


FIG. 3: Type 1 (full line, full line with circles) and type 2 (dashed line, dashed line with circles) solutions of the extended Hubbard model vs $W/4t$ for $U/4t = -30$ and $n = 0.01$. Dotted lines show axes of the coordination system. The dependence of $\bar{\mu}$ on W is indistinguishable in the scale of the picture from the dependence of $\bar{\mu}$ on U in Fig. 2 (apart from different thresholds for type 2 solutions), so it was not shown. In the inset the enlargement of the area near the origin of the coordination system is shown.

numerically the same, nevertheless they are two different solutions of two different types of pairing!

In the limit of large $|U|$ or large $|W|$ the solutions for Δ_0 and Δ_γ are symmetric or antisymmetric regarding to the change $n \rightarrow 2 - n$. For large, negative U (or W) and fixed W (or U) Δ_0 (Δ_γ) of "pure-s" (of "pure extended s") type 1 solution is symmetric, reaching maximum for the half-filled band, while Δ_γ (Δ_0) is antisymmetric: positive (or negative) for less than half-filled band and of opposite sign for more than half-filled band, crossing through 0 for $n = 1$. In the opposite limit U (or W) going to $+\infty$ the behavior of Δ_0 and Δ_γ in "type 1" solutions change to the reverse: Δ_0 (Δ_γ) becomes antisymmetric and Δ_γ (Δ_0) symmetric. The behavior vs n of type 2 solutions for U or $W \rightarrow -\infty$ is the same as behavior of respective "pure-s" or "pure extended s" type 1 solutions in the limit U or $W \rightarrow +\infty$. This is the correct behavior if the limiting, constant values reached by the type 1 solutions are to be identical to the type 2 limiting, constant solutions for every n . For smaller values of the parameters $|U|$, $|W|$ there is an area in parameter space of "type 2" solution, where both Δ_0 and Δ_γ are symmetric in the band, though of opposite sign.

A peculiarity of solutions is the existence of critical charge density n_c . For a given value of the fixed parameter (U or W) there exists n_c such that for n in the range $(n_c, 2 - n_c)$ the transition between the "pure (extended) s" part of one solution and the "constant" part of the same solution is no longer smooth, but both parts join in an non-continuous way: we have a first-order transition,

where Δ 's and derivative of $\bar{\mu}$ jump. Some approximate values of $n_c(U/4t, W/4t)$ for type 1 solution, given as a function of parameters for which the jump takes place, are: $n_c(-29.1, -30) \approx 0.0475$, $n_c(-9.1, -10) \approx 0.15$, $n_c(-2.75, -3.75) \approx 0.5$, $n_c(-1.1, -2) \approx 0.8$. We can see here that for $|W|$ large enough and attractive the jump takes place for $U \approx W$, as was stated before. The values of $|U|$ and $|W|$ required to obtain any given n_c are much larger in type 2 solution than in type 1 solution.

To complete the examination of the n -dependence let's notice that at half-filled band solutions fully separate and we obtain true pure-s solution, with $\Delta_\gamma = 0$ and no threshold for pairing and true pure extended s solution with $\Delta_0 = 0$ and threshold $W = -4t$ ($W \approx -3.24t$ for exact 2d density of states).²⁶

Another point to notice is that we can add the third and fourth solution to the two found, by changing Δ_0 and Δ_γ to $-\Delta_0$ and $-\Delta_\gamma$. The number of nontrivially-different solutions seems to depend on the number of coupled terms from the ansatz Eq. (10) and does not depend on the lattice dimensionality. In Fig. 1 there is a plot of threshold curves for simple cubic, three dimensional (3d) lattice. Their behavior is analogous to the 2d case. In particular the threshold line for the type-1 pairing goes through the point $(U, W) = (0, 0)$, even for small electron densities (except from $n = 0$). This does not contradict the fact that for $U = 0$ we have critical value for $|W|$ to bound electron pair in 3d. The existence of bound pairs is prerequisite for superconductivity in a dilute limit only in 2d¹⁹. A curve for two-electron bound pair in 3d can be obtained from Eqs. (11)-(13), by solving them for $n = 0$. This curve is also given in Fig. 1, plotted in a certain distance from other 3d curves for $n > 0$, in agreement with Refs.^{13,27}

There appears a question: which of the two solutions will be physically realized? The type 1 pairing has larger binding energy, higher critical temperature and lower free energy so this is the solution to be found even in the area of parameter space where both solutions exist. In this area care should be taken not to mix the two solutions especially for $U \approx W$, where the absolute values of solutions of type 1 become close to the respective values of solutions of type 2 and also in the limit of large negative U or W , where equations can easily yield type 2 solution numerically.

We must also remember that only the relative stability of two extended s-wave solutions was examined in the above considerations. The question of stability of another symmetry pairings, e.g. d - or p -wave, was not addressed at all. While p -wave pairing can be diminished by adding antiferromagnetic coupling to the Hamiltonian, d -wave can not. From Fig. 1 we can see that for large enough $|W|$, d -wave pairing can surely have bigger binding energy than second extended s-wave solution. As we know it can win the competition even with the first extended s-wave solution (with the lower free energy – see e.g.¹³). In establishing the detailed phase diagram we must thus take into account the competition of pairings with other

symmetries, including $s + d$ or $s + id$.

Another question is how physical is the first order transition found, isn't it just an artefact of the MFA, especially that it appears for larger n ? This question could be probably answered by numerical simulations. If this effect is physical it should have influence on the all superconducting properties of the superconductor with extended s -wave superconductivity. In particular one can ask whether the found first order transition could be an argument in favor of non-smooth crossover between BCS and local pairs limits in the models of extended s -wave superconductivity. It seems unlikely as we notice that $|U|$ and $|W|$ being the arguments of n_c cited before in the text, decrease for growing n_c while the BCS-Bose boundary (calculated from the Leggett's criterion,³⁰ i.e., that chemical potential crosses the bottom of the band) moves toward larger values of $|U|$ and $|W|$ with increasing electron density, so that the two boundaries do not coincide. Crossover boundaries for $n = 0$ and $n = 0.2$ are plotted in Fig. 1. There are two branches of crossover boundary corresponding to the two threshold lines. For $n = 0$ they coincide with the threshold lines, with increasing n they move left, towards larger and larger values of $|U|$ and $|W|$. Again, if other than s -wave symmetry pairing is realized, this problem is irrelevant.

The third issue concerns the possible phase separation for large, values of $|U|$ or $|W|$. This question was addressed by Hartree type analysis e.g. in the paper of Robaszkiewicz and Pawłowski²³, from where the phase boundaries shown in Fig. 4 come (solid lines). Under the lowest, horizontal line, for large n.n. attraction, we have a phase separation of normal state and electron droplets. In the area between the solid lines there is s -wave superconductivity (on-site only, denoted as SS) and above the upper solid line there is inhomogeneous phase separation of charge density waves (CDW) and superconductivity (CDW/SS). For the half filled band the ground state is CDW for $W > 0$ while CDW and superconductivity are degenerated for $W = 0$.

Our second superconducting s -wave solution does not enter this picture but for intermediate values of on-site attraction, Eq. (15) helps us to make an upper boundary for superconducting state, denoted by dashed lines in Fig. 4. Above this line no superconductivity exists. This way for small electron densities, for W large enough (above the critical value) a normal state is obtained (denoted as NO in the figure). With increasing n we can have a transition to SS and then to CDW/SS state. For certain larger W we can have NO-CDW/SS transition and for still larger W we obtain NO-CDW-CDW/SS transition. This way a phase diagram of Ref.²³ is substantially modified. Considering full extended s -wave superconducting solution, with order parameter depending on both on- and intersite interaction, changes phase

boundaries in Fig. 4 only in negligible way.

Let's note, that the described modification of the phase diagram takes place only for intermediate values of $|U|$. For larger values of $|U|$ or more precisely for $U < U_{as}$,

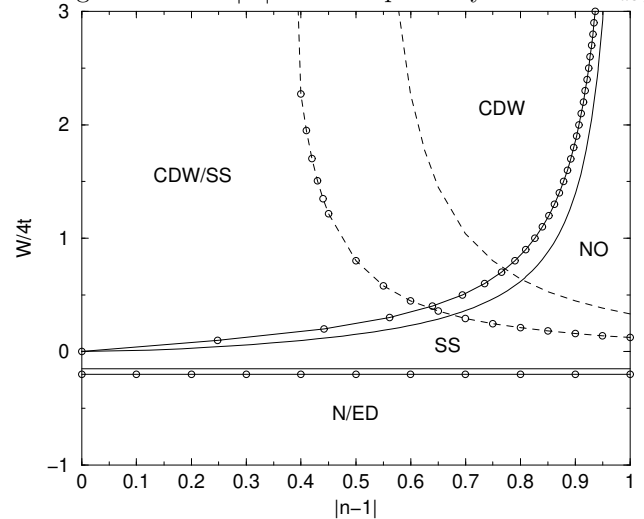


FIG. 4: The phase diagram of the extended Hubbard model solved in the mean-field approximation for $U/4t = -0.8$ (lines with no symbols) and $U/4t = -0.4$ (lines with circles). Full lines are taken from the paper of Robaszkiewicz and Pawłowski.²³ Dashed lines come from Eq. (15). N/ED denote phase separation between normal state and electron droplets, SS - superconductivity, CDW - charge density waves, CDW/SS - inhomogeneous phase separation between CDW and SS, NO - normal state.

where U_{as} was defined in connection with Fig. 1, s -wave superconductivity exists independently of W , and there is no normal phase area in the phase diagram.

In conclusion a mean-field criterion for existence of s -wave superconducting solution in the extended Hubbard model was calculated. The modified $W - n$ phase diagram was shown. A second s -wave solution was found and a threshold for its existence together with a full phase diagram in the UW plane were calculated. The second solution helped to answer the question why limits U (or W) = $\pm\infty$ are formally the same. (These results apply also to the two-electron bound states of the same symmetry). First-order transition in the extended s -wave solution was found and its possible implications on the crossover problem were discussed. The results may apply to all properties of the superconducting state of extended s -wave symmetry.

I acknowledge discussions with R. Micnas, P. Grzybowski and B. Tobijaszewska-Chorowska and support from the Foundation for Polish Science.

* karen@delta.amu.edu.pl

¹ J. Orenstein and A. J. Millis, Science 288, 468 (2000).

² D. J. Van Harlingen, Rev. Mod. Phys. **67**, 515 (1995).

³ M. Capone, M. Fabrizio, C. Castellani and E. Tossati, Science **296**, 2364 (2002).

⁴ J.-Y. Lin, P. L. Ho, H. L. Huang, P. H. Lin, Y.-L. Zhang, R.-C. Yu, C.-Q. Jin and H. D. Yang, Phys. Rev. B **67**, 052501 (2003).

⁵ P. Seneor, C.-T. Chen, N.-C. Yeh, R. P. Vasquez, L. D. Bell, C. U. Jung, M.-S. Park, H.-J. Kim, W. N. Kang and S.-I. Lee, Phys. Rev. B **65**, 012505 (2002).

⁶ Q. P. Li, B. E. C. Koltenbah and R. Joynt, Phys. Rev. B **48**, 437 (1993).

⁷ C. O'Donovan, D. Branch, J. P. Carbotte and J. S. Preston, Phys. Rev. B **51**, 6588 (1995).

⁸ K. A. Kouznetsov, A. G. Sun, B. Chen, A. S. Katz, S. R. Bahcall, John Clarke, R. C. Dynes, D. A. Gajewski, S. H. Han, M. B. Maple, J. Giapintzakis, J.-T. Kim and D. M. Ginsberg, Phys. Rev. Lett. **79**, 3050 (1997).

⁹ L. Alff, S. Meyer, S. Kleefisch, U. Schoop, A. Marx, H. Sato, M. Naito and R. Gross, Phys. Rev. Lett. **83**, 2644 (1999).

¹⁰ J. A. Skinta, T. R. Lemberger, T. Greibe and M. Naito, Phys. Rev. Lett. **88**, 207003 (2002).

¹¹ A. Biswas, P. Fournier, M. M. Qazilbash, V. N. Smolyanova, H. Balci and R. L. Greene, Phys. Rev. Lett. **88**, 207004 (2002).

¹² J. A. Skinta, M.-S. Kim, T. R. Lemberger, T. Greibe and M. Naito, Phys. Rev. Lett. **88**, 207005 (2002).

¹³ R. Micnas, J. Ranniger and S. Robaszkiewicz, Rev. Mod. Phys. **62**, 113 (1990).

¹⁴ N.-C. Yeh, C.-T. Chen, G. Hammerl, J. Mannhart, A. Schmehl, C. W. Schneider, R. R. Schulz, S. Tajima, K. Yoshida, D. Garrigus and M. Strasik, Phys. Rev. Lett. **87**, 087003 (2001).

¹⁵ W. Zhang and Z. D. Wang, Phys. Rev. B **65**, 144527 (2002).

¹⁶ A. Mourachkine, Physica C **323**, 137 (1999).

¹⁷ G. Deutscher, Nature **397**, 410 (1999).

¹⁸ P. Nozieres and S. Schmitt-Rink, J. Low Temp. Phys. **59**, 195 (1985).

¹⁹ M. Randeria, J.-M. Duan and L.-Y. Shieh, Phys. Rev. Lett. **62**, 981 (1989); Phys. Rev. B **41**, 327 (1990).

²⁰ F. Pistolesi and P. Nozieres, Phys. Rev. B **66**, 054501 (2002).

²¹ M. Bak and R. Micnas, Mol. Phys. Rep. **24**, 168 (1999), cond-mat/9909089.

²² M. Bak, Ph.D. thesis, A. Mickiewicz University, Poznań 1999.

²³ S. Robaszkiewicz and G. Pawłowski, Acta Phys. Pol. A **90**, 569 (1996).

²⁴ A. S. Blaer, H. C. Ren and O. Tchernyshyov, Phys. Rev. B **55**, 6035 (1997).

²⁵ R. Friedberg, T. D. Lee and H. C. Ren, Phys. Rev. B **50**, 10190 (1994).

²⁶ R. Micnas, J. Ranniger, S. Robaszkiewicz and S. Tabor, Phys. Rev. B **37**, 9410 (1988).

²⁷ P. Kornilovitch, cond-mat/0311195.

²⁸ C. Bastide, C. Lacroix and A. da Rosa Simoes, Physica C **159**, 347 (1989).

²⁹ A. Romano, C. Noce and R. Micnas, Phys. Rev. B **55**, 12640 (1997).

³⁰ A. J. Leggett in "Modern Trends in the Theory of Condensed Matter", eds. A. Pekalski and R. Przystawa (Springer-Verlag, Berlin, 1980).